Iğdır Üniversitesi Fen Bilimleri Enstitüsü Dergisi, 15(1), 330-342, 2025
Journal of the Institute of Science and Technology, 15(1), 330-342, 2025

ISSN: 2146-0574, eISSN: 2536-4618

Moleculer Biology and Genetic **DOI: 10.21597/jist.1526603**

Research Article

Received: 10.10.2024 **Accepted: 05.03.2024**

To Cite: Tülek, A. (2025). Biotechnological Potential of *Rheinheimera sp.* L-asparaginase: Heterologous Production and Its Role in Acrylamide Mitigation. *Journal of the Institute of Science and Technology*, 15(1), 330-342.

Biotechnological Potential of *Rheinheimera sp.* L-asparaginase: Heterologous Production and Its Role in Acrylamide Mitigation

Ahmet TÜLEK

Highlights:

- *Rs*ASNase was heterologously produced and purified
- The highest acrylamide mitigation was 51.3% using 100 U of the enzyme
- Docking analysis of the enzyme against L-asparagine was performed

Keywords:

- L-asparaginase
- *Rheinheimera sp.*
- Acrylamide mitigation
- Heterologous expression

ABSTRACT:

Acrylamide, a chemical contaminant found in foods, poses a significant health threat because of its toxic and carcinogenic properties. One of the most effective methods for reducing acrylamide is the application of L-asparaginase (L-ASNase) to decrease the asparagine content in foods before cooking or processing. In this study, L-ASNase (*Rs*ASNase) from *Rheinheimera sp.* was expressed heterologously in *Escherichia coli* Rosetta™2 (DE3) host cells. The enzyme was purified using Ni^{2+}-NTA affinity chromatography, yielding a specific activity of 392.2 U/mg and a purification fold of 4.0. Acrylamide reduction was assessed using a starch-L-asparagine model analyzed by high-performance liquid chromatography (HPLC). The highest acrylamide mitigation (52.3%) was achieved using 100 U of the enzyme after 120 min of incubation. Additionally, the three-dimensional structure of *Rs*ASNase was modeled using the ProMod3. Bioinformatics analyses, including docking studies, revealed interactions between the *Rs*ASNase enzyme's active site and the L-asparagine substrate, involving the amino acids THR162A, LYS242A, THR273A, LEU304A, and GLU305A. These findings showed that *Rs*ASNase has the potential for further development and application in biotechnological processes aimed at acrylamide mitigation.

Ahmet TÜLEK (**Orcid ID:** 0000-0003-1079-7837), Iğdır University, Vocational School of Health Services, Department of Patient Care Services, Iğdır, Türkiye
Corresponding Author: Ahmet TÜLEK, e-mail: ahmet.tulek@igdir.edu.tr

INTRODUCTION

Acrylamide (2-propenamide) is a toxic and carcinogenic molecule that forms during the frying and baking of carbohydrate-rich foods. This occurs through a nonenzymatic reaction between the amino group of L-asparagine (L-ASN) and the carbonyl group of reducing sugars. As a reactive unsaturated amide, acrylamide is characterized by its double bond, which predisposes it to form bonds with amino (-NH_2) and sulfhydryl (-SH) groups (Govindaraju et al., 2024). This toxic molecule is a white, odorless crystalline solid with a molecular weight of 71.08 g/mol. It melts at 84.5°C and boils at 192.6°C. As a polar compound, acrylamide readily dissolves in polar solvents such as water, methanol, and ethanol (Adimas et al., 2024). This molecule is one of the most common toxic agents found in foods. The presence of acrylamide in food was first identified in 2002, and it was discovered during the heating of starch-rich foods at high temperatures (Díaz-Ávila et al., 2023). Recent research has identified two widely accepted pathways for acrylamide formation: the Maillard reaction and the acrolein pathway. In the Maillard reaction, the α-amino group of free asparagine (L-ASN), which is naturally present in starch-rich foods, interacts with the carbonyl group of reducing sugars when processed at temperatures above 120°C (such as baking, roasting, and frying). This interaction results in the formation of acrylamide, with a key intermediate (Schiff base) being converting into acrylamide during the process (Lund & Ray, 2017). In the acrolein pathway, an acrolein compound forms when fats are heated to high temperatures, causing monoacylglycerol to break down into acrolein. Acrolein is first converted to acrylic acid via oxidation. The acrylic acid reacts with ammonia to produce acrylamide (Bachir et al., 2022). Proteins and amino acids serve as nitrogen sources for the amide groups in acrylamide. Amino acids not only contribute nitrogen to the formation of acrylamide but also play a role in the development of brown color and roasted flavor in baked foods, alongside the formation of aroma and color compounds found in cooked and roasted foods. These processes are associated with the Maillard reaction (Pandiselvam et al., 2024).

In 1994, the International Agency for Research on Cancer (IARC) identified acrylamide as a likely human carcinogen, categorizing it under Group 2A. Additionally, the Scientific Committee on Food (SCF) indicated in 2002 that acrylamide possesses genotoxic properties (Hogervorst & Schouten, 2022). Exposure to acrylamide varies among populations based on age and dietary preference. In Europe, the daily average acrylamide intake ranges from 0.14 to 1.31 µg/kg body weight, whereas in America, it ranges from 0.43 to 1.10 µg/kg body weight (Tardiff et al., 2010; Virk-Baker et al., 2014). Moreover, due to lower body weight and dietary preferences, it is estimated that children's dietary intake of acrylamide is 2-3 times higher than that of adults (Timmermann et al., 2021). Research in humans suggests a possible link between the consumption of acrylamide via diet and the development of specific cancers. These cancers include those of the kidney, endometrium, and ovaries (Filippini et al., 2022). Additionally, studies have suggested that acrylamide may have adverse effects on the nervous system and may lead to neurological disorders (Kopańska et al., 2022).

Numerous studies in the literature have been conducted to determine acrylamide levels in foods. According to current findings, approximately 50% of human exposure to acrylamide originates from potato products, whereas baked goods and bread account for approximately 20% of exposure (Keramat et al., 2011). Potato (*Solanum tuberosum*) is one of the most widely cultivated and consumed agricultural crops globally. Approximately 80% of the countries worldwide engage in potato cultivation, with annual production exceeding 300 million tons (Pedreschi et al., 2007). According to TURKSTAT (Turkish Statistical Institute) data from 2017, Türkiye produced 4750 tons of potatoes in 2016, harvested from a total area of 1.447.056 ha. Potato fries are widely consumed by millions of

people worldwide. Bakery products, such as bread and pastries, generally exhibit relatively low acrylamide levels, with the highest concentrations observed in the crust of bread, whereas breadcrumbs contain minimal acrylamide. Crispy bread, which contains significant amounts of acrylamide, is an exception to this trend (Ameur et al., 2024). Coffee is among the most consumed beverages globally, with daily consumption exceeding two billion cups worldwide (Lim et al., 2019). The primary coffee species used for beverage preparation are *Coffea arabica* and *Coffea canephora* (robusta). These two species are most commonly used in the coffee industry. Among its constituents, coffee contains bioactive compounds like caffeine, caffeic acid, and chlorogenic acid. These compounds contribute to the various health benefits of beverages (Makiso et al., 2024). Moreover, roasting coffee beans generates the toxic and carcinogenic compound acrylamide (Kocadağlı & Gökmen, 2022). The presence of acrylamide in widely consumed foods has heightened public health concerns and encouraged the development of strategies to reduce acrylamide formation in processed foods (Perera et al., 2021).

Various strategies have been implemented in the food industry to reduce the formation of carcinogenic acrylamide. These include controlling the temperature/time of heating processes, lowering pH levels, and regulating raw material storage temperatures (Maan et al., 2022). Additionally, additives such as calcium chloride and amino acids mitigate the formation of acrylamide. Moreover, pre-boiling potatoes before frying has been reported to effectively minimize acrylamide content (Ahmed & Mohammed, 2024; Bruno et al., 2024). The methods such as using raw materials with low reducing sugars and low L-ASN content have also been suggested for reducing acrylamide (Boyaci Gunduz, 2023). However, these practices are not widely adopted due to concerns over undesirable taste and appearance, as well as potential reductions in the nutritional value of foods (Hossein Abedini et al., 2024). Due to the impracticality of removing acrylamide from processed foods, researchers have focused on strategies to prevent its formation before cooking (Hendriksen et al., 2009). One measure adopted by food operators to reduce acrylamide content in foods is the use of asparaginase enzyme, as proposed in the European Commission Regulation of 2017. L-ASNase is an enzyme involved in preventing acrylamide formation. Notably, L-ASNase has emerged as a promising and effective strategy compared with other reduction methods because it does not compromise the sensory qualities of the product. By converting L-ASNase, a precursor of acrylamide, into aspartic acid and ammonia, this enzyme can significantly reduce acrylamide levels in foods. Applying it before frying or baking can reduce acrylamide formation by 96-99% (Gazi et al., 2023; Jia et al., 2021).

In this study, the L-ASNase enzyme previously cloned and characterized from *Rheinheimera* sp. by Yilmazer et al. was recombinantly produced by transferring it into *E. coli* Rosetta^{TM}2 (DE3) cells instead of *E. coli* BL-21 host cells (Yilmazer Aktar et al., 2023). Subsequently, it was tested for the first time for acrylamide mitigation, and bioinformatic docking analyses were conducted. The X-ray crystal structure of L-ASNase from *Rheinheimera* sp. (*Rs*ASNase) has not yet been characterized. However, based on the X-ray crystal structure of *E. coli* L-ASNase I (Lubkowski & Wlodawer, 2019; Yun et al., 2007), whose structure is known and most similar to *Rs*ASNase in terms of amino acid sequence, the L-ASN interaction site of *Rs*ASNase was determined using a homology model. The significant active site residues of *E. coli* L-ASNase I are Thr14, Thr91, Lys163, and Asp92 (Yun et al., 2007).

MATERIALS AND METHODS

The pET21a(+) plasmid containing the *Rheinheimera sp.* L-ASNase gene was obtained from Bauzyme (Türkiye) (Yilmazer Aktar et al., 2023). Nessler reagent was sourced from Merck for the experiments, and a Qiagen QIAwave Plasmid Miniprep Kit (USA) was used for plasmid isolation. The enzyme expression study employed the *E. coli* Rosetta™ 2(DE3) strain, which was acquired from Novagen in Germany. A protein marker (Precision Plus Protein™, 161-0373) was purchased from Bio-Rad (USA). All chemicals used were of analytical grade and were sourced from Merck (Germany), unless stated otherwise.

Transformation and expression of pET21a(+)-*Rs*ASNase

The pET21a(+)-*Rs*ASNase plasmid was transformed into $CaCl_2$-competent *E. coli* DH5α cells using the heat shock method at a ratio of 10 ng/50 µL (plasmid / competent cells). Following transformation, the cells were plated on LB (Luria Bertani) agar containing ampicillin (final concentration 100 µg/mL) and incubated overnight at 37°C. Plasmid isolation was performed from the resulting colonies. The pET21a(+)-*Rs*ASNase plasmid was then similarly transformed into competent *E. coli* Rosetta™ 2 (DE3) host cells for L-ASNase expression.

A single colony of *E. coli* Rosetta™ (DE3) harboring the *Rs*ASNase gene was inoculated into 10 mL of LB broth with 100 µg/mL ampicillin and incubated overnight at 37°C, shaking at 220 rpm. The following day, the culture was transferred at a 1/10 (v/v) ratio into 250 mL of LB broth containing 100 µg/mL ampicillin. The culture was then incubated at 37°C with shaking at 220 rpm until the OD_{600} reached 0.45-0.6. Isopropyl-1-thio-β-D-galactoside (IPTG) was added to a final concentration of 1 mM, and incubation was continued for an additional 5 h. The obtained culture obtained was subsequently used for purification.

Purification of *Rs*ASNase

To purify *Rs*ASNase, the 250 mL expression culture was centrifuged at 4500 rpm for 10 min at 4°C. The supernatant was discarded, and the pellet was resuspended in PBS buffer (pH 7.4) at a volume of 1 mL per gram of pellet. Lysozyme was introduced to achieve a final concentration of 1 mg/mL, and the mixture was kept at 4°C for 30 min. After incubation, the cells were sonicated on ice with 20-second pulses followed by 10-second intervals for a total of 5 min. The lysate was then centrifuged at 9000 rpm for 35 min at 4°C. The *Rs*ASNase, which contains a C-terminal 6xHistidine tag, was purified using a HisTrapFF™ (immobilized metal affinity chromatography, IMAC) column on an AKTA Prime Plus Purification System. Prior to loading 5 mL of the enzyme-containing supernatant, the column was equilibrated with 20 mM imidazole (pH 7.4). The supernatant was filtered through a 0.45 µm filter, loaded onto the column, and washed with 25 mM imidazole (pH 7.4). *Rs*ASNase was then eluted with 400 mM imidazole (pH 7.4). The purified enzyme was subjected to buffer exchange and concentration using an Amicon® Ultra-15 Centrifugal Filter Unit (Merck) equipped with 10,000 MWCO and resuspended in 50 mM Tris HCl (pH 7.5). Protein concentrations were measured using a BCA Protein Assay Kit (Pierce™, Thermo Fisher Scientific) and enzyme purity was evaluated using SDS-PAGE (12% polyacrylamide gel).

*Rs*ASNase activity

The activity experiments were conducted according to the method reported by Özdemir et al. (Özdemir et al., 2022). L-ASNase activity was determined by measuring the released ammonia using Nessler reagent. L-ASN was used as the substrate. A reaction mixture containing 2.5 µL (0.003 mg *Rs*ASNase) and 347.5 µL of 50 mM Tris-HCl (with 50 µL of L-ASN) was incubated at 45 °C for 10

min. The reaction was stopped by adding 150 µL of 1.5 M trichloroacetic acid (TCA) and centrifuged at 11.000 rpm for 15 min. For the Nessler reagent assay, 1400 µL of distilled water and 150 µL of supernatant were used. After incubating the samples at room temperature for 15 min, the amount of released ammonia was measured at 450 nm using a UV spectrophotometer. A unit (U) of L-ASNase activity is defined as the amount of enzyme that produces 1 µmol of ammonia per min under the specified conditions. A control experiment was also conducted without the free enzyme.

Acrylamide mitigation

The potential of *Rs*ASNase for acrylamide mitigation was assessed according to the method reported by Özdemir et al. (2023). HPLC (Agilent 1260 Infinity Diode Array Detector (G4212B)) was used for this purpose. To induce acrylamide formation, 2% starch and 2% L-ASN were mixed in a 1 mL sample and incubated for 120 min. A 0.5 mL aliquot was then taken, and the acrylamide formation reaction was carried out using a thermoreactor (Spectroquant TR 420) at 170°C for 5 min. For acrylamide mitigation, enzyme concentrations of 20, 40, 50, 70, 90 and 100 unit (U) were used. An acrylamide (Acrylamide (purity > 99.9%) from M/s Sigma Aldrich) standard curve was established on the HPLC (Acrylamide standard linear graphic range: 250 ppb-20 ppm). The mobile phase consisted of 95% (0.1% phosphoric acid in water) and 5% acetonitrile. The column temperature was maintained at 40°C, the injection volume was 10 µL, the flow rate was 1 mL/min, detection was set at 206/4 nm with a reference wavelength of 400/100 nm, and an Acegenerix 5C18 (4.6x250 nm) column with a particle size of 5 µm was used. Acrylamide mitigation was calculated as a percentage using the following formula:

$$Acrylamide\ mitigation\ (\%) = \frac{(Ab - Ae)}{(Ae)} x100$$

In reactions in which enzymes are not used, the amount of acrylamide formed is denoted as *Ab* (blank). Conversely, *Ae* represents the quantity of acrylamide produced by the enzyme treatment.

Molecular docking analysis of *Rs*ASNase

The amino acid sequence of the *Rs*ASNase protein (UniProtKB: A0A2D5S0K3) was obtained from the UniProt database (Bateman et al., 2023). The length of this protein sequence from *Rheinheimera sp.* is 341 amino acids. According to the UniProt database, the three-dimensional structure of *Rs*ASNase was not obtained in any experimental studies. Therefore, *in silico* methods were used to obtain the three-dimensional homology structure (homo-tetramer) of *Rs*ASNase. In addition to structure modeling applications such as AlphaFold (Jumper et al., 2021), SWISS-MODEL (Waterhouse et al., 2018) is an application that uses the template of the crystal structure as a reference to predict protein models. Accordingly, SWISS-MODEL and ProMod3 were used to predict the 3D homology structure of *Rs*ASNase (Waterhouse et al., 2018). For the multiple sequence alignment of *Rs*ASNase and 2HIM (Yun et al., 2007) template amino acid sequences, the BLOSUM-62 algorithm with the Chimera application was used. Chimera (Pettersen et al., 2004) and Autodock Vina (Eberhardt et al., 2021; Trott & Olson, 2010) were used to dock the L-ASN ligand to the active site of the *Rs*ASNase homology model. The PLIP application was used to identify the protein-ligand interaction profiles (Adasme et al., 2021).

RESULTS AND DISCUSSION

In *E. coli* Rosetta^{TM}2 (DE3) host cells, the purified *Rs*ASNase achieved 19.7% activity, a purification fold of 392.2 U/mg (**Table 1**). The obtained enzyme was used for acrylamide mitigation.

Yilmazer et al. reported *Rs*ASNase production in *E. coli* BL-21 cells, obtaining 1.47-fold purification, a specific activity of 161.36 U/mg, and a yield of 8.96% (Yilmazer Aktar et al., 2023). The discrepancies in enzyme production between these two studies could be attributed to differences in the expression system, the presence of rare codons (Codon Adaptation Index (CAI) value), and the purification procedures employed (Özdemir et al., 2022; Tegel et al., 2010).

Table 1. Purification process of *Rs*ANSase.

Purification phases	Volume (mL)	Total Protein (mg)	Total Activity (U)	Specific Activity (U/mg)	Purification (Fold)	Activity yield (%)
Cell free extract	10.0	28.3	2785.6	98.4	1.0	100
Ni^{2+}-NTA purification	4.8	2.5	743.2	297.3	3.0	26.7
Ultrafiltration	2.4	1.4	549.1	392.2	4.0	19.7

After purification, *Rs*ASNase was detected at approximately ~37 kDa on SDS-PAGE (**Fig. 1**).

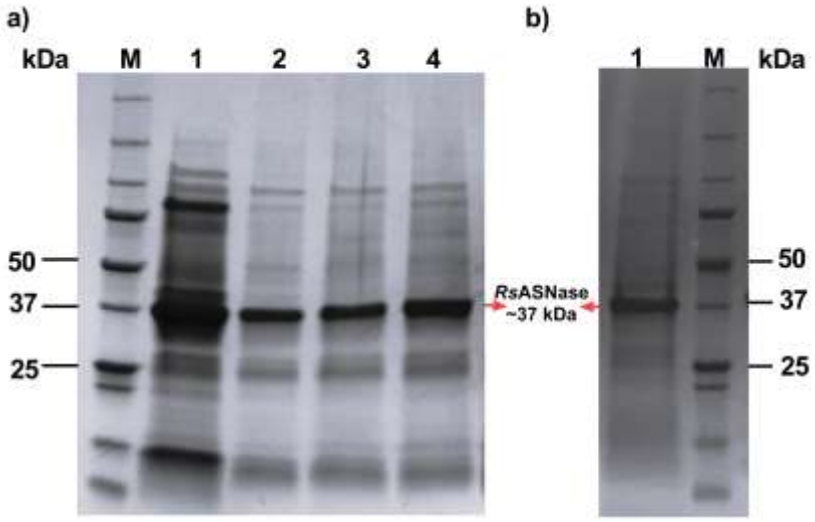

Fig. 1. After purification, SDS-PAGE analysis of *Rs*ASNase. a) Fraction profile of the enzyme. M: marker; Lane 1: cell-free extract, Lines 2, 3 and 4: 100, 200 and 400-mM imidazole, respectively. b) Concentrated enzyme. M: marker, Lane 1: *Rs*ASNase (37 kDa)

The acrylamide reduction reaction using the *Rs*ASNase-starch-L-ASN model is illustrated in **Fig. 2**. Initially, a standard curve for acrylamide (correlation: 0.99997; retention time: 3.431) was established using HPLC (**Fig. 2a**). Following 120-min reactions, the highest acrylamide reduction was achieved using 100 U of the enzyme (**Fig. 2b**). Acrylamide reduction increased with the enzyme units over the reaction process. Specifically, acrylamide reductions of 4.98%, 24.2%, 36.2%, %38.8, 47.9%, and 51.3% were observed with the use of 20, 40, 50, 70, 90, and 100 U of the enzyme, respectively.

The enzymatic reduction of acrylamide in food products has become a major focus because of its associated health risks. This process has received considerable attention as a potential solution to mitigate these risks. Several studies have explored the efficacy of L-ASNase enzymes from various microbial sources under different reaction conditions to mitigate acrylamide formation in potato-based snacks. Shahana et al. (2023) demonstrated a 50% reduction in acrylamide content in potato chips using 50 U/mL L-ASNase from *Streptomyces katangensis* at 40°C for 30 min (Shahana Kabeer et al., 2023).

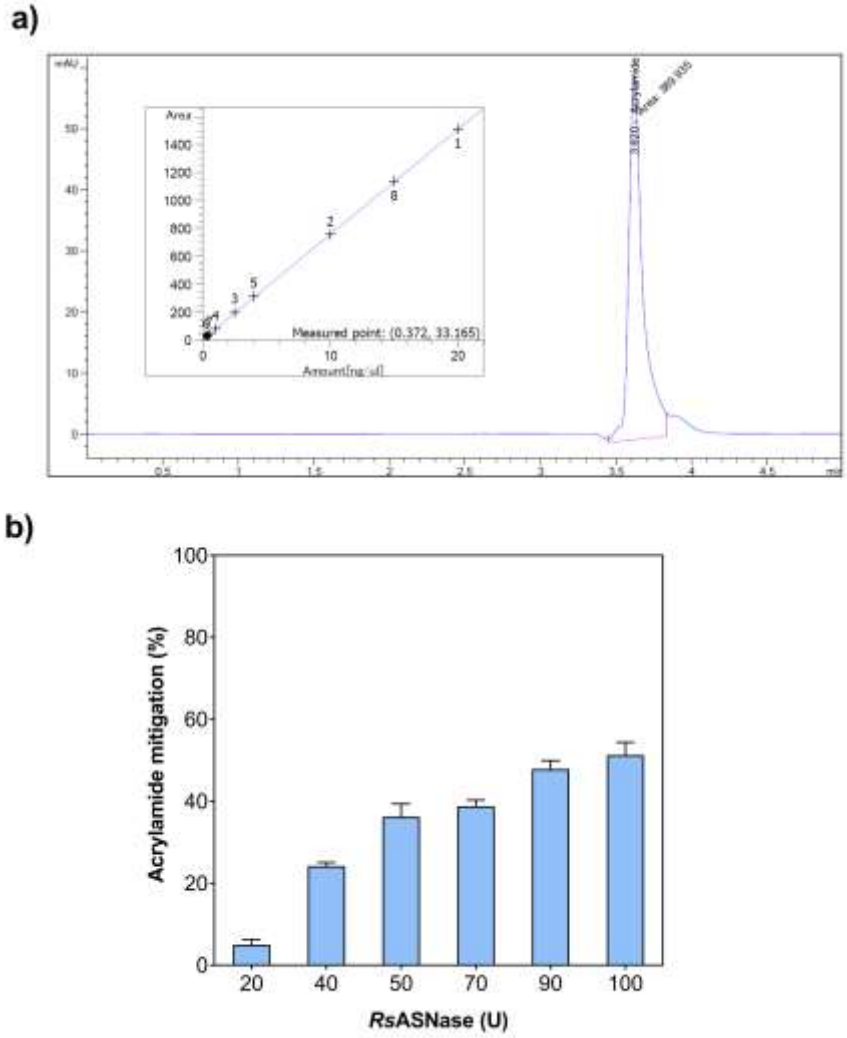

Fig. 2. Acrylamide mitigation analysis of *Rs*ASNase. a) Acrylamide standard curve generated using HPLC. b) Effects of different enzyme concentrations on acrylamide mitigation

Similarly, Chi et al. (2021) achieved a 65.09% reduction with 40 U/mL of L-ASNase levels from *Mycobacterium gordonae* at 37°C for 30 min (Chi et al., 2021). Jiao et al. (2020) reported a 55.9% reduction in *Acinetobacter soli* treated with L-ASNase at 37°C for 30 min (Jiao et al., 2020). Moreover, Zuo et al. (2015) observed an 80.5% reduction in French fries using L-ASNase from *Thermococcus zilligii* at 80°C for 4 min (Zuo et al., 2015). Khalil et al. (2021) applied L-ASNase from *Penicillium crustosum* to achieve an 80.7% reduction in acrylamide content in light-roasted coffee beans at 35°C for 60 min (Khalil et al., 2021). Recently, Patel et al. (2024) reported a substantial 74% reduction using *B. licheniformis* UDS-5 L-ASNase at 30°C for 30 min in French fries (Joshi et al., 2024). Notably, Özdemir et al. (2023) achieved the highest reduction rate of 93% in a starch-L-ASN food model system using 1.5 U/mL enzyme at 55°C for 60 min (Özdemir et al., 2024). These findings underscore the diverse enzymatic capabilities of different microbial sources and reaction conditions in mitigating acrylamide formation, thereby highlighting the potential of enzymatic approaches as effective food processing strategies to ensure product safety and quality.

The amino acid sequence similarity between *Rs*ASNase and *E. coli* L-ASNase I was determined to be 68.84%. The conserved residues between the amino acids of the *Rs*ASNase and 2HIM structures are shown in **Figure 3** with highlighted gray zones. In particular, it has been reported that the

important active site residues of *E. coli* L-ASNase I are Thr14, Thr91, Lys163, and Asp92 amino acids (Yun et al., 2007).

Fig. 3. Amino acid sequence alignment of the *Rs*ASNase homology model and 2HIM template crystal structure

Table 2. Protein (*Rs*ASNase homology model, Chain A) ligand (L-ASN) interaction profile.

Hydrogen Bonds			
Index	**Residue (A*)**	**AA**	**Distance (Å)**
1	162A	THR	2.02
2	242A	LYS	3.11
3	273A	THR	2.44
4	304A	LEU	3.06
5	305A	GLU	1.61
Salt Bridge			
Index	**Residue (A*)**	**AA**	**Distance (Å)**
1	242A	LYS	1.99

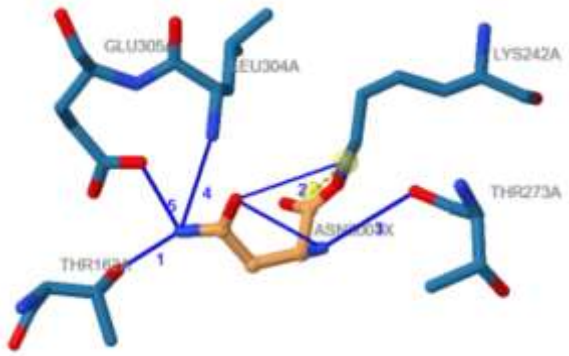

*Chain A.
Blue lines: hydrogen bonds, yellow lines and balls represent the salt bridge.
THR: threonine, LYS: lysine, LEU: leucine, GLU: glutamic acid.

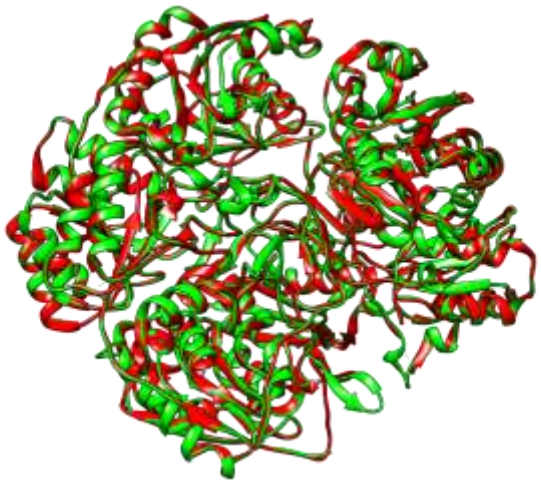

Figure 4. Superimposed representations of the *Rs*ASNase homology model (green) and 2HIM template crystal structure (red)

In this present study, in silico studies revealed the interactions between THR162A, LYS242A, THR273A, LEU304A, GLU305A *Rs*ASNase, and L-ASN. Significantly, the THR residues and the salt bridge of the LYS residue with the asparagine ligand are presented in **Table 2**. The X-ray crystal structure PDB: 2HIM (Yun et al., 2007) was used as a template for the homology structure of *Rs*ASNase. The RMSD difference between the homology model obtained and the reference template was calculated to be 0.278 Ångstrom (Å) for A chains. Superimposed images of the *Rs*ASNase homology model and the 2HIM template crystal structure are shown in **Figure 4**.

CONCLUSION

In this study, the *Rs*ASNase enzyme was heterologously expressed in *E. coli* Rosetta™ 2(DE) cells and was subsequently tested for its applicability in food products using a starch-L-ASN model to assess acrylamide reduction. The application of 100 U of the enzyme resulted in an impressive 52.3% reduction in the acrylamide content within 120 min, indicating significant potential for industrial biotechnological applications. Additionally, bioinformatics studies were conducted to analyze the interactions between amino acids in the enzyme's catalytic site and L-ASN using docking analyses. The results revealed that the *Rs*ASNase catalytic site retains a conserved structure similar to that of other. Future research should focus on enzyme engineering and the development of immobilized enzyme systems to further enhance the catalytic activity, reusability, and stability of *Rs*ASNase. These advancements will not only optimize the enzyme’s performance but also contribute to its commercial viability in food processing industries, ensuring the production of safer food products by reducing acrylamide content.

ACKNOWLEDGEMENTS

I would like to thank Bauzyme Company (Türkiye) for providing the pET21a(+)-*Rs*ASNaz plasmid.

REFERENCES

Adasme, M. F., Linnemann, K. L., Bolz, S. N., Kaiser, F., Salentin, S., Haupt, V. J., & Schroeder, M. (2021). PLIP 2021: expanding the scope of the protein–ligand interaction profiler to DNA and RNA. *Nucleic Acids Research*, 49(W1), W530–W534. https://doi.org/10.1093/nar/gkab294.

Adimas, M. A., Abera, B. D., Adimas, Z. T., Woldemariam, H. W., & Delele, M. A. (2024). Traditional food processing and acrylamide formation: A review. *Heliyon*, 10(9), e30258. https://doi.org/10.1016/j.heliyon.2024.e30258.

Ahmed, Z. A. & Mohammed, N. K. (2024). Investigating influencing factors on acrylamide content in fried potatoes and mitigating measures: a review. *Food Production, Processing and Nutrition*, 6(1), 1–16. https://doi.org/10.1186/s43014-023-00212-6.

Ameur, H., Tlais, A. Z. A., Paganoni, C., Cozzi, S., Suman, M., Di Cagno, R., Gobbetti, M., & Polo, A. (2024). Tailor-made fermentation of sourdough reduces the acrylamide content in rye crispbread and improves its sensory and nutritional characteristics. *International Journal of Food Microbiology*, 410, 110513. https://doi.org/10.1016/j.ijfoodmicro.2023.110513.

Bachir, N., Haddarah, A., Sepulcre, F., & Pujola, M. (2022). Formation, mitigation, and detection of acrylamide in foods. *Food Analytical Methods*, 15(6), 1736–1747. https://doi.org/10.1007/s12161-022-02239-w/tables/3.

Bateman, A., Martin, M. J., Orchard, S., Magrane, M., Ahmad, S., Alpi, E., Bowler-Barnett, E. H., Britto, R., Bye-A-Jee, H., Cukura, A., Denny, P., Dogan, T., Ebenezer, T. G., Fan, J., Garmiri, P., da Costa Gonzales, L. J., Hatton-Ellis, E., Hussein, A., Ignatchenko, A., & Zhang, J. (2023). UniProt: The universal protein knowledgebase in 2023. *Nucleic Acids Research*, 51(D1), D523–D531. https://doi.org/10.1093/nar/gkac1052.

Boyaci Gunduz, C. P. (2023). Formulation and processing strategies to reduce acrylamide in thermally processed cereal-based foods. *International Journal of Environmental Research and Public Health*, 20(13). https://doi.org/10.3390/ijerph20136272.

Bruno, F., Ledbetter, M., Davies, B., Riedinger, L., Blidi, S., Sturrock, K., McNamara, G., Montague, G., & Fiore, A. (2024). Effect of ultrasound and additives treatment as mitigation strategies to reduce acrylamide formation in potato crisps on industrial scale. *LWT- Food Science and Technology*, 197, 115876. https://doi.org/10.1016/j.lwt.2024.115876.

Chi, H., Chen, M., Jiao, L., Lu, Z., Bie, X., Zhao, H., & Lu, F. (2021). Characterization of a novel l-asparaginase from *Mycobacterium gordonae* with acrylamide mitigation potential. *Foods*, 10(11), 2819. https://doi.org/10.3390/foods10112819/s1.

Díaz-Ávila, W. Y., Villarreal-Archila, S. M., & Castellanos-Galeano, F. J. (2023). Acrylamide in starchy foods subjected to deep-frying, 20 years after its discovery (2002-2022): a patent review. *F1000Research*, 12. https://doi.org/10.12688/f1000research.140948.2.

Eberhardt, J., Santos-Martins, D., Tillack, A. F., & Forli, S. (2021). AutoDock Vina 1.2.0: New docking methods, expanded force field, and python bindings. *Journal of Chemical Information and Modeling*, 61(8), 3891–3898. https://doi.org/10.1021/acs.jcim.1c00203.

Filippini, T., Halldorsson, T. I., Capitão, C., Martins, R., Giannakou, K., Hogervorst, J., Vinceti, M., Åkesson, A., Leander, K., Katsonouri, A., Santos, O., Virgolino, A., & Laguzzi, F. (2022). Dietary acrylamide exposure and risk of site-specific cancer: A systematic review and dose-response meta-analysis of epidemiological studies. *Frontiers in Nutrition*, 9, 875607. https://doi.org/10.3389/fnut.2022.875607.

Gazi, S., Göncüoğlu Taş, N., Görgülü, A., & Gökmen, V. (2023). Effectiveness of asparaginase on reducing acrylamide formation in bakery products according to their dough type and properties. *Food Chemistry*, 402, 134224. https://doi.org/10.1016/j.foodchem.2022.134224.

Govindaraju, I., Sana, M., Chakraborty, I., Rahman, M. H., Biswas, R., & Mazumder, N. (2024). Dietary acrylamide: A detailed review on formation, detection, mitigation, and its health impacts. *Foods*, 13(4). https://doi.org/10.3390/foods13040556.

Hogervorst, J. G. F. & Schouten, L. J. (2022). Dietary acrylamide and human cancer; even after 20 years of research an open question. *The American Journal of Clinical Nutrition*, 116(4), 846. https://doi.org/10.1093/ajcn/nqac192.

Hossein Abedini, A., Vakili Saatloo, N., Salimi, M., Sadighara, P., Alizadeh Sani, M., Garcia-Oliviera, P., Prieto, M. A., Saeed Kharazmi, M., & Mahdi Jafari, S. (2024). The role of additives on acrylamide formation in food products: a systematic review. *Critical Reviews in Food Science and Nutrition*, 64(10), 2773–2793. https://doi.org/10.1080/10408398.2022.2126428.

Jia, R., Wan, X., Geng, X., Xue, D., Xie, Z., & Chen, C. (2021). Microbial L-asparaginase for application in acrylamide mitigation from food: Current research status and future perspectives. *Microorganisms*, 9(8). https://doi.org/10.3390/microorganisms9081659.

Jiao, L., Chi, H., Lu, Z., Zhang, C., Chia, S. R., Show, P. L., Tao, Y., & Lu, F. (2020). Characterization of a novel type I L-asparaginase from *Acinetobacter soli* and its ability to inhibit acrylamide formation in potato chips. *Journal of Bioscience and Bioengineering*, 129(6), 672–678. https://doi.org/10.1016/j.jbiosc.2020.01.007.

Joshi, D., Patel, H., Suthar, S., Patel, D. H., & Kikani, B. A. (2024). Evaluation of the efficiency of thermostable l-asparaginase from *B. licheniformis* UDS-5 for acrylamide mitigation during preparation of French fries. *World Journal of Microbiology and Biotechnology*, 40(3), 1–15. https://doi.org/10.1007/s11274-024-03907-1.

Jumper, J., Evans, R., Pritzel, A., Green, T., Figurnov, M., Ronneberger, O., Tunyasuvunakool, K., Bates, R., Žídek, A., Potapenko, A., Bridgland, A., Meyer, C., Kohl, S. A. A., Ballard, A. J., Cowie, A., Romera-Paredes, B., Nikolov, S., Jain, R., Adler, J., & Hassabis, D. (2021). Highly accurate protein structure prediction with AlphaFold. *Nature*, 596(7873), 583–589. https://doi.org/10.1038/s41586-021-03819-2.

Keramat, J., LeBail, A., Prost, C., & Jafari, M. (2011). Acrylamide in baking products: A review Article. *Food and Bioprocess Technology*, 4(4), 530–543. https://doi.org/10.1007/s11947-010-0495-1.

Khalil, N. M., Rodríguez-Couto, S., & El-Ghany, M. N. A. (2021). Characterization of *Penicillium crustosum* L-asparaginase and its acrylamide alleviation efficiency in roasted coffee beans at non-cytotoxic levels. *Archives of Microbiology*, 203(5), 2625–2637. https://doi.org/10.1007/s00203-021-02198-6.

Kocadağlı, T. & Gökmen, V. (2022). Formation of acrylamide in coffee. *Current Opinion in Food Science*, 45, 100842. https://doi.org/10.1016/j.cofs.2022.100842.

Kopańska, M., Łagowska, A., Kuduk, B., & Banaś-Ząbczyk, A. (2022). Acrylamide neurotoxicity as a possible factor responsible for inflammation in the cholinergic nervous system. *International Journal of Molecular Sciences*, 23(4). https://doi.org/10.3390/ijms23042030.

Lim, L. T., Zwicker, M., & Wang, X. (2019). Coffee: One of the most consumed beverages in the world. *Comprehensive Biotechnology*, 275–285. https://doi.org/10.1016/b978-0-444-64046-8.00462-6.

Lubkowski, J. & Wlodawer, A. (2019). Geometric considerations support the double-displacement catalytic mechanism of L-asparaginase. *Protein Science*, 28(10), 1850–1864. https://doi.org/10.1002/pro.3709.

Lund, M. N. & Ray, C. A. (2017). Control of Maillard reactions in foods: Strategies and chemical mechanisms. *Journal of Agricultural and Food Chemistry*, 65(23), 4537–4552. https://doi.org/10.1021/acs.jafc.7b00882.

Maan, A. A., Anjum, M. A., Khan, M. K. I., Nazir, A., Saeed, F., Afzaal, M., & Aadil, R. M. (2022). Acrylamide formation and different mitigation strategies during food processing – A review. *Food Reviews International*, 38(1), 70–87. https://doi.org/10.1080/87559129.2020.1719505.

Makiso, M. U., Tola, Y. B., Ogah, O., & Endale, F. L. (2024). Bioactive compounds in coffee and their role in lowering the risk of major public health consequences: A review. *Food Science & Nutrition*, 12(2), 734. https://doi.org/10.1002/fsn3.3848.

Özdemir, F. İ., Didem Orhan, M., Atasavum, Z. T., & Tülek, A. (2022). Biochemical characterization and detection of antitumor activity of L-asparaginase from thermophilic *Geobacillus kaustophilus* DSM 7263^{T}. *Protein Expression and Purification*, 199. https://doi.org/10.1016/j.pep.2022.106146.

Özdemir, F. İ., Tülek, A., Karaaslan, B., & Yildirim, D. (2024). Evaluation of multi-walled carbon nanotubes bearing aldehyde groups of different lengths for the immobilization of *Geobacillus kaustophilus* L-asparaginase. *Molecular Catalysis*, 555, 113903. https://doi.org/10.1016/j.mcat.2024.113903.

Pandiselvam, R., Süfer, Ö., Özaslan, Z. T., Gowda, N. N., Pulivarthi, M. K., Charles, A. P. R., Ramesh, B., Ramniwas, S., Rustagi, S., Jafari, Z., & Jeevarathinam, G. (2024). Acrylamide in food products: Formation, technological strategies for mitigation, and future outlook. *Food Frontiers*, 5(3), 1063–1095. https://doi.org/10.1002/fft2.368.

Pedreschi, F., León, J., Mery, D., Moyano, P., Pedreschi, R., Kaack, K., & Granby, K. (2007). Color development and acrylamide content of pre-dried potato chips. *Journal of Food Engineering*, 79(3), 786–793. https://doi.org/10.1016/j.jfoodeng.2006.03.001.

Perera, D. N., Hewavitharana, G. G., & Navaratne, S. B. (2021). Comprehensive study on the acrylamide content of high thermally processed foods. *BioMed Research International*, 2021. https://doi.org/10.1155/2021/6258508.

Pettersen, E. F., Goddard, T. D., Huang, C. C., Couch, G. S., Greenblatt, D. M., Meng, E. C., & Ferrin, T. E. (2004). UCSF Chimera-A visualization system for exploratory research and analysis. *Journal of Computational Chemistry*, 25(13), 1605–1612. https://doi.org/10.1002/jcc.20084.

Shahana Kabeer, S., Francis, B., Vishnupriya, S., Kattatheyil, H., Joseph, K. J., Krishnan, K. P., & Mohamed Hatha, A. A. (2023). Characterization of L-asparaginase from *Streptomyces koyangensis* SK4 with acrylamide-minimizing potential in potato chips. *Brazilian Journal of Microbiology*, 54(3), 1645–1654. https://doi.org/10.1007/s42770-023-00967-7.

Tardiff, R. G., Gargas, M. L., Kirman, C. R., Leigh Carson, M., & Sweeney, L. M. (2010). Estimation of safe dietary intake levels of acrylamide for humans. *Food and Chemical Toxicology*, 48(2), 658–667. https://doi.org/10.1016/j.fct.2009.11.048.

Tegel, H., Tourle, S., Ottosson, J., & Persson, A. (2010). Increased levels of recombinant human proteins with the *Escherichia coli* strain Rosetta (DE3). *Protein Expression and Purification*, 69(2), 159–167. https://doi.org/10.1016/j.pep.2009.08.017.

Timmermann, C. A. G., Mølck, S. S., Kadawathagedara, M., Bjerregaard, A. A., Törnqvist, M., Brantsæter, A. L., & Pedersen, M. (2021). A review of dietary intake of acrylamide in humans. *Toxics*, 9(7). https://doi.org/10.3390/toxics9070155/s1.

Trott, O. & Olson, A. J. (2010). AutoDock Vina: Improving the speed and accuracy of docking with a new scoring function, efficient optimization, and multithreading. *Journal of Computational Chemistry*, 31(2), 455–461. https://doi.org/10.1002/jcc.21334.

Virk-Baker, M. K., Nagy, T. R., Barnes, S., & Groopman, J. (2014). Dietary Acrylamide and Human Cancer: A Systematic Review of Literature. *Nutrition and Cancer*, 66(5), 774. https://doi.org/10.1080/01635581.2014.916323.

Waterhouse, A., Bertoni, M., Bienert, S., Studer, G., Tauriello, G., Gumienny, R., Heer, F. T., De Beer, T. A. P., Rempfer, C., Bordoli, L., Lepore, R., & Schwede, T. (2018). SWISS-MODEL: homology modelling of protein structures and complexes. *Nucleic Acids Research*, 46(W1), W296–W303. https://doi.org/10.1093/nar/gky427.

Yilmazer Aktar, B., Georgakis, N., Labrou, N., Turunen, O., & Binay, B. (2023). Comparative structural and kinetic study for development of a novel candidate L-asparaginase based pharmaceutical. *Biochemical Engineering Journal*, 191, 108806. https://doi.org/10.1016/j.bej.2023.108806.

Yun, M. K., Nourse, A., White, S. W., Rock, C. O., & Heath, R. J. (2007). Crystal structure and allosteric regulation of the cytoplasmic *Escherichia coli* L-Asparaginase I. *Journal of Molecular Biology*, 369(3), 794–811. https://doi.org/10.1016/j.jmb.2007.03.061.

Zuo, S., Zhang, T., Jiang, B., & Mu, W. (2015). Reduction of acrylamide level through blanching with treatment by an extremely thermostable L-asparaginase during French fries processing. *Extremophiles*, 19(4), 841–851. https://doi.org/10.1007/s00792-015-0763-0.